W-band Gyro-BWO with a Four-stage Depressed Collector

Liang Zhang*, Wenlong He, Craig R. Donaldson, Adrian W. Cross, Alan D. R. Phelps, Paul McElhinney and Kevin Ronald
SUPA, Department of Physics, University of Strathclyde, Glasgow, G4 0NG, Scotland, UK
* Email: liang.zhang@strath.ac.uk

Abstract: An energy recovery system using a four-stage depressed collector was simulated and designed to improve the overall efficiency of the W-band gyrotron backward wave oscillator (gyro-BWO) at the University of Strathclyde. The spent beam information was exported from the simulation of the gyro-BWO using the 3D PIC code MAGIC. The geometry of the depressed collector was optimized using a genetic algorithm to achieve the optimum overall recovery efficiency for specific parameters of the spent beam. Secondary electron emissions and their effects on the recovery efficiency and the backstreaming of the electrons from the collector region were simulated. The heat power distribution on the electrodes was also simulated to avoid the "hot spot".

Keywords: Gyro-BWO, Depressed collector, Energy recovery, Secondary electron emission.

1. INTRODUCTION

Gyro-BWOs are gyrodevices based on the electron cyclotron maser instability. They are with wide frequency tuneability and high power capability from the microwave to terahertz frequency range. The gyro-BWOs have attracted many interests for their potential applications such as radar, communication, and plasma diagnostics. Gyro-BWOs based on helically corrugated waveguides can achieve even wider frequency tuning range and higher efficiency. The helically corrugated waveguide couples two modes in the circular waveguide to generate a new operating eigen-mode which has large group velocity in low axial wavenumber range to make it less sensitive to the electron beam energy[4]. Gyro-BWOs based on helically corrugated waveguides have demonstrated excellent results in X-band and Ka-band [1-3]. A W-band gyro-BWO currently being built at the university of Strathclyde was predicted to have a 3 *dB* frequency bandwidth of 84–104 *GHz*, output power of 10 *kW* with an electronic efficiency of 17% [5, 6].

The gyro-BWOs suffer slightly lower interaction efficiency when comparing with the gyromonotron and gyroklystron. In gyro-BWOs, the amplitude of the RF field increases as the RF wave traveling to the entrance. In the entrance, the amplitude of RF field reaches its maximum and it causes an abrupt electron bunching, while the RF field is weak in the exit of the interaction region resulting in a weak beam-wave interaction. The electrons lose less energy to the wave and the efficiency is low. Several methods have been developed to improve the efficiency of beam-wave interaction. One is to change the profile of the waveguide, such as employing slot structure [7], helical structure [1-6] and slice structure [8]. The other way is using tapered magnetic field or tapered wall radius instead of the constant ones [9, 10]. However, once the electronic tube has been established, the electronic efficiency would be fixed too. Another way to increase the overall efficiency is to recover energy using single or multi-stage depressed collectors from the spent beam. It has been proved that it is an efficiency way to improve the overall efficiency of microwave tubes, such as conventional klystrons, BWOs and TWTs [11, 12].

However, it is still a challenge to employ multi-stage depressed collectors in gyrotron devices as the electrons always have large transverse velocity which makes them hard to be sorted.

In this paper, an energy recovery system using multi-stage depressed collectors to recover the energy from the spent beam was designed for a W-band gyro-BWO. This gyro-BWO was based on the helically corrugated waveguide and a cusp electron gun. The experimental setup and the schematic of the W-band gyro-BWO are shown in Fig. 1 and Fig. 2. The cusp electron gun was designed to produce an axis-encircling annular beam of 40 *kV*, 1.5 *A* with a beam alpha of 1.65 [13-15]. The microwave radiation was generated in the helically corrugated interaction region and then the spent electron beam entered into the collection region. To extract the radiation out of the interaction region, a side-wall coupler that achieves a good transmission over the operating frequency range was designed and placed at the upstream of the interaction region. A Bragg reflector acting as a microwave short in the operating frequency range at the end of the helical waveguide, was used to reflect the radiation back into the interaction region.

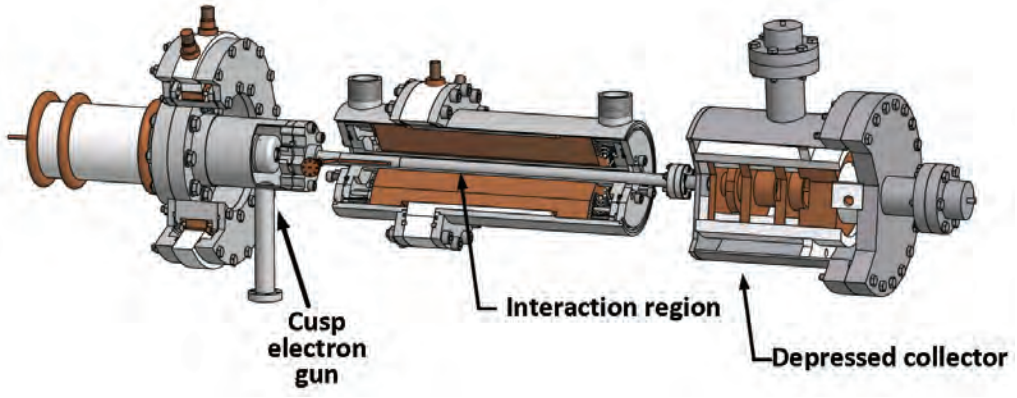

Fig. 1 The experimental setup of the W-band gyro-BWO.

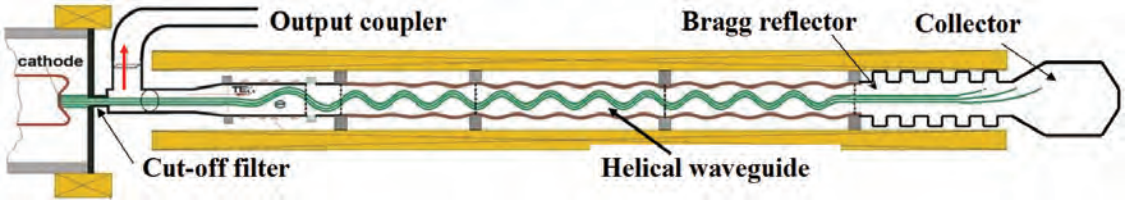

Fig. 2 The schematic of the W-band gyro-BWO.

2. PRINCIPLE OF THE DEPRESSED COLLECTOR

Depressed collectors are passive converters that can transfer the kinetic energy of the spent electrons into potential electric energy. “Depressed” means that the collector has a depressed potential as compared with the main body of the tube. The electrons lose their kinetic energy when passing through the retarding electrostatic field and finally land on the collector surface with a significant reduction in kinetic energy. They produce a loop current which results in a

power recovery from the spent electrons. The collected power by a depressed collector can be written as

$$P_{col} = \sum_n V_n I_n \tag{1}$$

where n is the number of stages and V_n, I_n are potentials and collected current on the nth-stage electrode, respectively. By introducing a depressed collector with a collection efficiency of η_{col}, the overall efficiency of the microwave tube η_{tot} with an electronic efficiency η_e can be calculated using

$$\eta_{tot} = \frac{P_{out}}{P_b - P_{col}} = \frac{\varepsilon_{out}\eta_e}{1-\eta_{col}(1-\eta_e)} \tag{2}$$

where ε_{out} , the output efficiency, is the ratio of the output microwave power and generated microwave power in the cavity. For those inherently low efficiency high power microwave devices, depressed collectors with efficiencies higher than 80% can significantly improve the overall efficiencies. For a moderately efficient source with an electronic and collection efficiency of 30% and 80%, respectively, with the use of depressed collection the overall efficiency could be increased to 61.4% when ε_{out} = 0.9, increasing the overall efficiency by a factor of 2.

3. SIMULATION OF THE DEPRESSED COLLECTOR

The design of a depressed collector involves several issues like determining the potentials and the geometry of the electrodes to reach the optimum collection efficiency, the effect of the secondary electrons and the heat distribution on the electrodes.

The collection efficiency of a depressed collector is mainly dependent on the potentials on the electrodes and the geometry of the electrodes. When specifying a stage number, the optimum potentials on the electrodes can be evaluated by the energy distribution of the spent electron beam which was exported from the simulation of the gyro-BWO using the 3D PIC code MAGIC. It should be noted that, in the calculation, it was assumed that all the electrons were collected on the electrodes without consideration of secondary emissions. To avoid backstreaming, the minimum electrode potential was set to be the minimum energy of electrons, and the maximum potential was set to be the electron beam voltage which was 40 *kV* in the considered W-band gyro-BWO. The energy distribution of the spent electron beam is shown as Fig. 3 and the collection efficiency at different stage number is shown in Table 1.

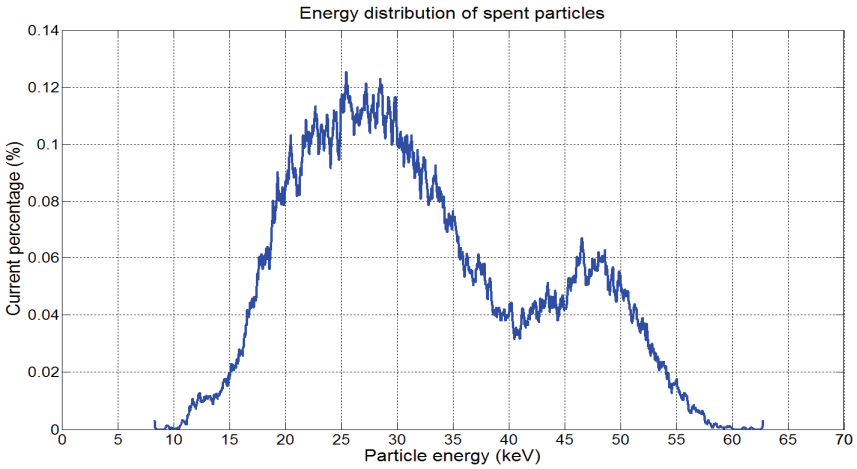

Fig. 3 The energy distribution of the spent electron beam

Tab. 1 Collection efficiency at different stage number

No.	**Potentials on electrodes (kV) (relative to ground voltage)**							**Collection efficiency**
1	-9.24	-----	-----	-----	-----	-----	-----	28.8%
2	-9.24	-25.70	-----	-----	-----	-----	-----	63.6%
3	-9.24	-22.14	-36.57	-----	-----	-----	-----	75.7%
4	-9.24	-19.55	-27.31	-40.00	-----	-----	-----	82.5%
5	-9.24	-18.86	-24.96	-30.78	-40.00	-----	-----	85.7%
6	-9.24	-16.98	-22.14	-27.22	-32.66	-40.00	-----	87.5%
7	-9.24	-16.82	-21.33	-25.47	-29.53	-34.23	-40.00	88.7%

The depressed collectors with different geometries of the electrodes were simulated by 3D PIC code MAGIC and the parameters for the geometries were optimized by the genetic algorithm. A detail description of the simulation flow chart can be found in paper [16]. In the optimization, the evaluation function was chosen as

$$\eta_{eva} = \eta_{col} - W\eta_{back} \tag{3}$$

where η_{back} was the percentage of the backstreaming electrons, and W was the weight. In the simulation, W was chosen as 1.5. The optimization was run with the magnetic field of 1.75 T and an optimum collection efficiency of 78.7% was achieved. It was 3.8% lower than the ideal collection efficiency which assumes all the spent electrons were sorted perfectly. That was because not all the electrons were collected by the electrodes and a small proportion were observed to become backstreaming in the simulation. The trajectories of the spent electrons are shown in Fig. 4.

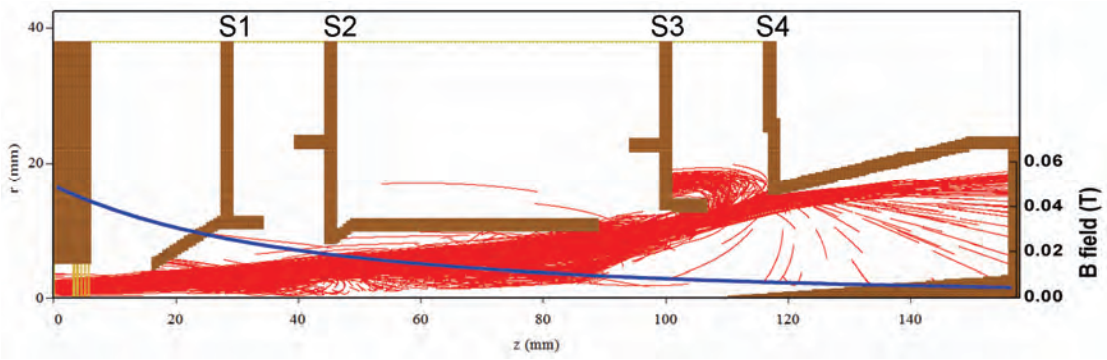

Fig. 4 The trajectories of the spent electron beam.

The secondary electrons have several negative effects on high power microwave devices. First of all, secondary electrons carrying velocities with opposite direction to the primaries will be accelerated by the electrostatic field in the collection region and some of them will become backstreaming. The secondary electrons absorb energy from the electrostatic field and decrease the collection efficiency. Secondly, the backstreaming entered into the RF interaction region, which will generate noise on the microwave output and decrease the performance of the microwave tube. Thirdly, in high average power devices, the backstreaming may contribute an additional thermal power on the thermally stressed waveguide structure. Thus in depressed collectors, it is essential to reduce the current of secondary electrons to be as low as possible. Secondary electrons are generally divided into two classes. The first class is the true secondary electrons (TSEs) which are knocked out from the surface of the material due to the bombardment of the primary electrons. The other class is the backscattered electrons (BSEs) including the re-diffused electrons and the elastic scattering electrons.

Secondary electron emission models were applied in the simulation of the depressed collector to investigate the effect of the secondary electrons. The TSE yield function in MAGIC is based on that by Thomas [17]. However, MAGIC also allows users to define their own SEY functions and the energy distribution function for TSEs by using the command "EMISSION SECONDARY." In our simulation, different formulas were tested including the Vaughan's [18], Furman's [19] and Thomas's equations and the effect on the collection efficiency was studied.

The scattering process of the BSEs in MAGIC is carried out by the ITS code. The "BACKSCATTER"option in MAGIC allows ITS to be invoked automatically to simulate the emission of both the rediffiused and backscattered elastic electrons. The TSE and BSE models used in the MAGIC simulations were discussed in detail in the paper [20]. Table 2 is a summary of the simulation results with consider different TSE models and the BSEs. The optimum geometry of the four-stage depressed collector as well as the trajectories of the primary electron, true secondary electrons and the backscattered electrons is shown in Fig. 5.

The collection efficiencies and the backstreaming rate of the W-band gyro-BWO were simulated in the whole frequency tuning range by the optimized configuration of the designed four-stage depressed collector. The collection efficiencies achieved were about 70% and the backstreaming rate was lower than 7% in the working frequency band. Thus an overall efficiency of 40% can be achieved.

Tab. 2 Collection efficiency at different stage number.

Cases	TSE model	Collection efficiency	Percentage of backstreaming
without TSEs, without BSEs	-----	75.7%	4.79%
with TSEs, without BSEs	Vaughan	71.1%	4.79%
	Furman	68.9%	4.80%
	Thomas	73.0%	4.80%
without TSEs, with BSEs	-----	73.9%	4.89%
with TSEs, with BSEs	Vaughan	69.0%	4.89%
	Furman	66.8%	4.91%
	Thomas	71.0%	4.90%

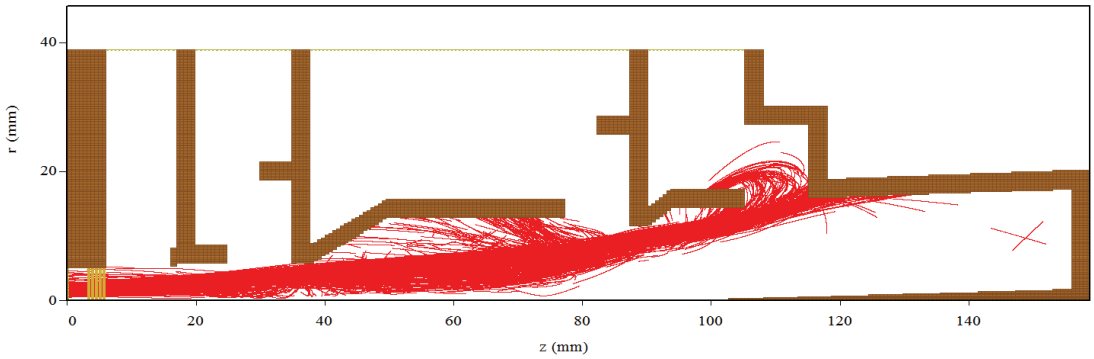

(a) Trajectories of the primary electrons.

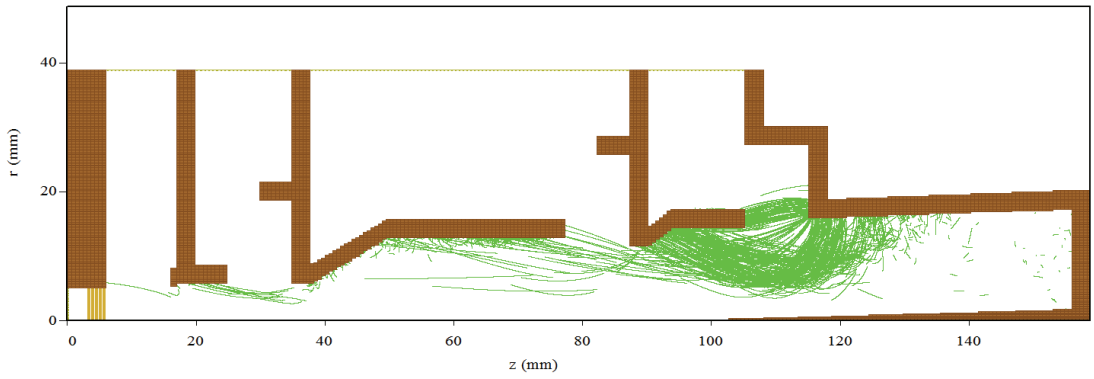

(b) Trajectories of the true secondary electrons.

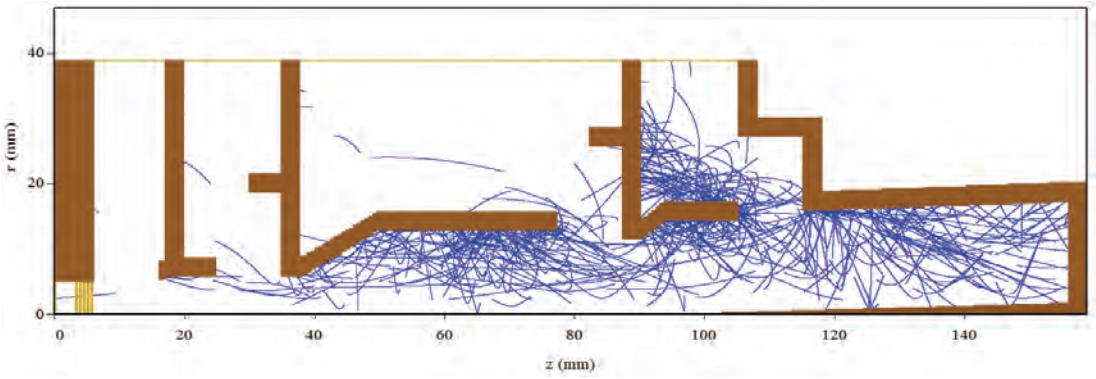

(c) Trajectories of the backscattered electrons.

Fig. 5 Trajectories of the electrons in the depressed collector (using Vaughan's formulas).

The heat power dissipation on the electrodes is another important issue in designing the depressed collector. Although the kinetic energy of the spent electrons reduced significantly when they passed through the retarded electric field, the heat due to the power of the remaining kinetic energy of the spent electrons when they struck the surface of the electrodes was still large, for our case, it could be up to 20 keV. The spent electrons with such high kinetic energy could damage the surface of electrodes in the form of a "hot spot" and could reach the thermal stress threshold of the collector material.

To design effective cooling system for the collector electrodes, the distribution of the heat power dissipated on the surface of the electrodes needs to be evaluated. In MAGIC, there is no straightforward way to get the heat power on the electrodes directly. However, it provides a command "OBSERVE COLLECTED POWER" to observe the overall heat dissipation on a conductor. To obtain the heat power distribution on the surface of the electrodes, the electrodes were divided into a large number of small conductors both in the azimuthal direction and the *z* direction and the heat power dissipated in each of these conductors was individually measured, thus an approximate heat power distribution was obtained. The heat power densities on the conductors calculated from the collected electric power and the area of the conductors. In the simulation, the maximum heat density was ~240W/cm^2. It is lower than the thermal stress threshold of the copper material thus the generation of "hot spots" can be avoided.

Reference

[1] W. He, K. Ronald, A. R. Young, A. W. Cross, A. D. R. Phelps, C. G. Whyte, E. G. Rafferty,J. Thomson, C. W. Robertson, D. C. Speirs, S. V. Samsonov, V. L. Bratman, and G. G. Denisov, "Gyro-BWO experiments using a helical interaction waveguide", *IEEE Trans. Electron Devices*, 52, 5, 839–844 (2005).

[2] W. He, A. W. Cross, A. D. R. Phelps, K. Ronald, C. G. Whyte, S. V. Samsonov, V. L. Bratman, and G. G. Denisov, "Theory and simulations of a gyrotron backward wave oscillator using a helical interaction waveguide", *Appl. Phys. Lett.*, 8, 091504 (2006).

[3] V. L. Bratman, G. G. Denisov, V. N. Manuilov, S. V. Samsonov, and A. B. Volkov, “Development of helical-waveguide gyro-devices based on low-energy electron beams”, *Int. Conf. Infrared and Millimeter Waves, France*, 5–105 (2001).

[4] Gregory G. Denisov, Vladimir L. Bratman, Alan D. R. Phelps, and Sergei V. Samsono, "Gyro-TWT with a Helical Operating Waveguide: New Possibilities to Enhance Efficiency and Frequency Bandwidth", *IEEE Trans. Plasma Sci.*, 26, 3, 508-518 (1998).

[5] W. He, C. R. Donaldson, F. Li, L. Zhang, A. W. Cross, A. D. R. Phelps, K. Ronald, C. W. Robertson, C. G. Whyte, and A. R. Young, “W-band gyro-devices using helically corrugated waveguide and cusp gun: design, simulation and experiment”, *T. S. T.*, 4, 9-19 (2011).

[6] W. He, C. R. Donaldson, L. Zhang, K. Ronald, A. D. R. Phelps, and A. W. Cross, “Numerical Simulation of a Gyro-BWO with a Helically Corrugated Interaction Region, Cusp Electron Gun and Depressed Collector”, *Numerical Simulations / Book 2*, Intech publisher (2011).

[7] N. C. Chen, C. F. Yu, and T. H. Chang, “A TE_{21} Second-harmonic Gyrotron Backward-wave Oscillator with Slotted Structure”, *Phys. Plasmas*, 14, 123105 (2007).

[8] Q. S. Wang, D. B. McDermott, and N. C. Luhmann, “Demonstration of Marginal Stability Theory by a 200-kW Second-Harmonic Gyro-TWT Amplifier”, *Phys. Rev. Lett.*, 75, 4322 (1995).

[9] G. S. Nusinovich, and O. Dumbrajs, “Theory of gyro-backward wave oscillators with tapered magnetic field and waveguide cross section”, *IEEE Trans. Plasma Sci.*, 24, 3, 620-629 (1996).

[10] Mark T. Walter, Ronald M. Gilgenbach, John W. Luginsland, Jonathan M. Hochman, J. I. Rintamaki, Reginald L. Jaynes, Y. Y. Lau, and Thomas A. Spencer, “Effects of tapering on gyrotron backward-wave oscillators”, *IEEE Trans. Plasma Sci.*, 24, 3, 636-647 (1996).

[11] W. Neugebauer, and T. G. Mihran, "A ten-stage electrostatic depressed collector for improving klystron efficiency", *IEEE Trans. Electron Devices*, 19, 1, 111- 121 (1972).

[12] J. D. Wilson, E. G. Wintucky, K. R. Vaden, D. A. Force, I. L.Krainsky, R. N. Simons, N. R. Robbins, W. L. Menninger, D. R. Dibb, and D. E. Lewis, "Advances in Space Traveling-Wave Tubes for NASA Missions", *Proceedings of the IEEE*, 95, 10, 1958-1967 (2007).

[13] W. He, C. G. Whyte, E. G. Rafferty, A. W. Cross, A. D. R. Phelps, K. Ronald, A. R. Young, C. W. Robertson, D. C. Speirs, and D. H. Rowlands, “Axis-encircling electron beam generation using a smooth magnetic cusp for gyrodevices”, *Appl. Phys. Lett.*, 93, 121501 (2008).

[14] C. R. Donaldson, W. He, A. W. Cross, A. D. R. Phelps, F. Li, K. Ronald, C. W. Robertson, C. G. Whyte, A. R. Young, and L. Zhang, “Design and numerical optimization of a cusp-gun-based electron beam for millimeter-wave gyro-devices”, *IEEE Trans. Plasma Sci.*, 37, 2153–2157 (2009).

[15] C. R. Donaldson, W. He, A. W. Cross, F. Li, A. D. R. Phelps, L. Zhang, K. Ronald, C. W. Robertson, C. G. Whyte, and A. R. Young, “A Cusp Electron Gun for Millimeter Wave Gyro-Devices”, *Appl. Phys. Lett.*, 96, 141501 (2010).

[16] L. Zhang, W. He, A. W. Cross, A. D. R. Phelps, K. Ronald, and C. G. Whyte, “Design of an energy recovery system for a gyrotron backward-wave oscillator”, *IEEE Trans. Plasma Sci.*, 37, 3, 390-394 (2009).

[17] MAGIC User’s Manual, *Mission Res. Corp.*, Newington, VA (2002).

[18] M. Vaughan, “Secondary emission formulas”, *IEEE Trans. Electron Devices*, 40, 4, 830 (1993).

[19] M. A. Furman and M. T. Pivi, "Probabilistic Model for the Simulation of Secondary Electron Emission", *Phys. Rev. ST Accel. Beams*, 5, 12, 124404 (2002).

[20] L. Zhang, W. He, A. W. Cross, A. D. R. Phelps, K. Ronald, and C. G. Whyte, “Numerical Optimization of a Multistage Depressed Collector With Secondary Electron Emission for an X-band Gyro-BWO”, *IEEE Trans. Plasma Sci.*, 37, 12, 2328-2334 (2009).